EARTHQUAKE ENGINEERING AND STRUCTURAL DYNAMICS, VOL. 25, 1195–1209 (1996)

TIME-HARMONIC VIBRATION OF AN INCOMPRESSIBLE LINEARLY NON-HOMOGENEOUS HALF-SPACE

GRIGORI MURAVSKII AND VALERY OPERSTEIN
Faculty of Civil Engineering, Technion, 32000 Haifa, Israel

SUMMARY

In this paper, time-harmonic axisymmetric vibration of an incompressible viscoelastic half-space having shear modulus linearly increasing with depth is studied. The half-space is subjected to a vertical time-harmonic load on its surface. Numerical results concerning surface displacements due to a point force are given for the case of non-zero shear modulus at the surface. Hankel's transforms of the solutions have an infinite number of poles lying on the real axis of the complex plane in the non-dissipative case. A suitable contour of integration is used to avoid all the singularities. Calculations are performed for the dynamic as well as for the static case. In addition, vertical vibrations of a rigid disk on the considered half-space are investigated, and the influence of the non-homogeneity on the dynamic stiffness of the loaded area is demonstrated.

KEY WORDS: time-harmonic vibration; non-homogeneous half-space; vertical point force; Hankel's transformation; material damping; rigid disk problem

INTRODUCTION

The non-homogeneous incompressible half-space with shear modulus varying linearly with depth was suggested as a soil model by Gibson.[1] He has also shown that such a half-space has a similarity with well-known Winkler's base in the case when the shear modulus is equal to zero at the surface of the half-space. Further investigations of the corresponding static problems were done by many authors (e.g. References 2–4). The axisymmetric time-harmonic problem was studied by Awojobi,[5,6] who constructed a solution using the confluent hypergeometric functions. For the case of zero surface shear modulus, he gave an approximate solution of the problem for a rigid circular body interacting with the half-space at low and high frequencies. Note that the assumption of zero surface modulus simplifies significantly the solution but confines the practical application of the model. In fact, the presence of a structure on the surface of the soil leads to an initial static pressure that results in non-zero shear modulus in the vicinity of the structure footing.

The main purpose of this paper is to study the action of a time-harmonic surface vertical load on the incompressible viscoelastic linearly non-homogeneous half-space in the case of non-zero shear modulus at the surface of the half-space. Such a half-space, although without damping, was considered in References 7–9 from the standpoint of free vibrations, i.e. characteristics of surface waves of Rayleigh type were determined. When solving the corresponding problem for given forces, difficulties are connected with an infinite number of poles of integrands in the integral representation of the solution. We avoid these difficulties by using the proper choice of the path of integration. Various dynamic problems for non-homogeneous bases were studied numerically by many authors, by means of dividing the non-homogeneous medium into a system of layers with constant properties.[10–15] These methods can lead to inaccurate results caused by reflection of waves at surfaces of discontinuity of properties and at the lower boundary that the numerical solutions require. The solution obtained in the present paper can be used for evaluation of the accuracy of numerical methods developed to treat dynamic problems in layered viscoelastic media.

CCC 0098–8847/96/111195–15
© 1996 by John Wiley & Sons, Ltd.
Received 8 November 1995
Revised 20 May 1996

In addition to studying the action of the vertical surface harmonic force, vertical vibrations of a rigid circular disk are studied in the paper. Calculations are performed by dividing the contact area into annular rings, assuming that the load amplitude is constant over the width of each annular ring. Presented numerical results demonstrate the influence of the non-homogeneity on the dynamic stiffness of the loaded area. For the static stiffness and for the real parts of the dynamic stiffness, the differences between results corresponding to the non-homogeneous half-space, and to the homogeneous half-space with the same shear modulus as that of the non-homogeneous half-space at the depth of the disk radius, are not significant. The main effect of the non-homogeneity results in the significant decrease of the imaginary part of the dynamic stiffness, compared to the homogeneous half-space, and consequently in the decrease of damping.

BASIC EQUATIONS

The equations of motion of an isotropic elastic medium in a cylindrical co-ordinate system for the axisymmetric case have the following form:

$$\rho\frac{\partial^2 u_r}{\partial t^2}=\frac{\partial\sigma_{rr}}{\partial r}+\frac{\partial\sigma_{zr}}{\partial z}+\frac{\sigma_{rr}}{r}-\frac{\sigma_{\vartheta\vartheta}}{r}$$
$$\rho\frac{\partial^2 u_z}{\partial t^2}=\frac{\partial\sigma_{rz}}{\partial r}+\frac{\partial\sigma_{zz}}{\partial z}+\frac{\sigma_{rz}}{r} \tag{1}$$

where r, ϑ, z are cylindrical co-ordinates; ρ is the density; σ_{ij} $(i, j = r, \vartheta, z)$ are the components of the stress tensor; u_r, u_z denote displacements in the directions of the co-ordinate lines ($u_\vartheta = 0$); and t is time. Using Hooke's law and the expressions for the components of the strain tensor results in

$$\sigma_{rr}=\lambda e+2G\frac{\partial u_r}{\partial r},\qquad \sigma_{\theta\theta}=\lambda e+2G\frac{u_r}{r}$$
$$\sigma_{zz}=\lambda e+2G\frac{\partial u_z}{\partial z},\qquad \sigma_{zr}=G\left(\frac{\partial u_z}{\partial r}+\frac{\partial u_r}{\partial z}\right) \tag{2}$$

where the dilatation, e, and Lamé's coefficient, λ, are introduced:

$$e=\frac{\partial u_r}{\partial r}+\frac{u_r}{r}+\frac{\partial u_z}{\partial z},\qquad \lambda=\frac{2G\nu}{1-2\nu} \tag{3}$$

in which ν is Poisson's ratio. Consider the harmonic motion with the dependence on time in the form $\exp(i\omega t)$ where ω is the circular frequency and $i=\sqrt{-1}$. Assuming that the shear modulus depends only on the co-ordinate z and Poisson's ratio is constant, we obtain the following equations for amplitudes (we keep for amplitudes the same notation as for displacements):

$$G\left(\nabla^2 u_r-\frac{u_r}{r^2}\right)+\frac{G}{1-2\nu}\frac{\partial e}{\partial r}+\frac{\partial G}{\partial z}\left(\frac{\partial u_z}{\partial r}+\frac{\partial u_r}{\partial z}\right)+\rho\omega^2 u_r=0$$
$$G\nabla^2 u_z+\frac{G}{1-2\nu}\frac{\partial e}{\partial z}+2\frac{\partial G}{\partial z}\left(\frac{\partial u_z}{\partial z}+\frac{\nu e}{1-2\nu}\right)+\rho\omega^2 u_z=0 \tag{4}$$

where

$$\nabla^2=\frac{\partial^2}{\partial r^2}+\frac{1}{r}\frac{\partial}{\partial r}+\frac{\partial^2}{\partial z^2}$$

It is assumed at this stage that $\nu < \frac{1}{2}$; when $\nu \to \frac{1}{2}$ the addendums with the value $1-2\nu$ in the denominator stay bounded because $e \to 0$. A solution of equations (4) can be expressed in the following form:

$$U_r = \int_0^\infty q(z,k) J_1(kr)\,\mathrm{d}k, \qquad U_z = \int_0^\infty w(z,k) J_0(kr)\,\mathrm{d}k \tag{5}$$

where $J_0(kr)$ and $J_1(kr)$ are Bessel functions, $q(z, k)$ and $w(z, k)$ are unknown functions that should be found using equations of motion (4) and corresponding boundary conditions. Note that the similar form of the solution with exponential functions for $q(z, k)$, $w(z, k)$ is widely used for homogeneous half-spaces and layers.[15] For a non-homogeneous half-space representation (5) was used by Vrettos.[16] Substitution of expressions (5) in equations (4) results in the following system of equations for q and w:

$$\begin{aligned} &G\frac{\mathrm{d}^2q}{\mathrm{d}z^2} + \frac{\mathrm{d}G}{\mathrm{d}z}\frac{\mathrm{d}q}{\mathrm{d}z} + \left(\rho\omega^2 - \frac{Gk^2}{\tau^2}\right)q - G\frac{1-\tau^2}{\tau^2}k\frac{\mathrm{d}w}{\mathrm{d}z} - \frac{\mathrm{d}G}{\mathrm{d}z}kw = 0 \\ &G\frac{\mathrm{d}^2w}{\mathrm{d}z^2} + \frac{\mathrm{d}G}{\mathrm{d}z}\frac{\mathrm{d}w}{\mathrm{d}z} + \tau^2(\rho\omega^2 - Gk^2)w + G(1-\tau^2)k\frac{\mathrm{d}q}{\mathrm{d}z} + \frac{\mathrm{d}G}{\mathrm{d}z}(1-2\tau^2)kq = 0 \end{aligned} \tag{6}$$

where

$$\tau^2 = \frac{1-2\nu}{2(1-\nu)} = \frac{G}{\lambda + 2G} = \frac{C_\mathrm{p}^2}{C_\mathrm{s}^2} \tag{7}$$

Here C_p and C_s are velocities of the compression and shear waves, respectively; this relation is constant for the considered case of non-homogeneity (Poisson's ratio is constant). Equations (6) coincide with the equations from Reference 16. The dilatation for solution (5) has the following form:

$$e = \int_0^\infty \left(kq + \frac{\partial w}{\partial z}\right) J_0(kr)\,\mathrm{d}k \tag{8}$$

Consider stress amplitudes (corresponding to solution (5)) that are needed for fitting the boundary conditions on planes $z = \text{const}$:

$$\begin{aligned} \sigma_{zz} &= \frac{G}{\tau^2}\int_0^\infty \left[\frac{\mathrm{d}w}{\mathrm{d}z} + qk(1-2\tau^2)\right] J_0(kr)\,\mathrm{d}k \\ \sigma_{rz} &= G\int_0^\infty \left(\frac{\mathrm{d}q}{\mathrm{d}z} - kw\right) J_1(kr)\,\mathrm{d}k \end{aligned} \tag{9}$$

Consider another form of these expressions:

$$\sigma_{zz} = \int_0^\infty (\hat{e} - 2kGq) J_0(kr)\,\mathrm{d}k, \qquad \sigma_{rz} = \int_0^\infty (\hat{\chi} - 2kGw) J_1(kr)\,\mathrm{d}k \tag{10}$$

where

$$\hat{e} = G\left(kq + \frac{\partial w}{\partial z}\right)/\tau^2, \qquad \hat{\chi} = G\left(\frac{\mathrm{d}q}{\mathrm{d}z} + kw\right) \tag{11}$$

The value $\hat{e}$ remains limited also for the incompressible material; also the value $\hat{\chi}$ is associated with the curl of the displacement field. We write equations (6) with the introduced quantities $\hat{e}$ and $\hat{\chi}$ and add the

definition (11) to obtain the following system of first-order differential equations:

$$
\begin{aligned}
\frac{d\hat{\chi}}{dz} &= k\hat{e} + 2k\frac{dG}{dz}w - \rho\omega^2 q \\
\frac{d\hat{e}}{dz} &= k\hat{\chi} + 2k\frac{dG}{dz}q - \rho\omega^2 w \\
\frac{dq}{dz} &= \frac{\hat{\chi}}{G} - kw \\
\frac{dw}{dz} &= \tau^2\frac{\hat{e}}{G} - kq
\end{aligned}
\tag{12}
$$

These equations allow us to carry out the calculations for the compressible ($\tau \neq 0$) as well as for the incompressible case ($\tau = 0$).

Suppose that for $z = z_0$ amplitudes of axisymmetric normal stresses $\sigma_{zz}(r)$ are given, whereas tangential stresses are equal to zero. Using equations (10) and properties of Hankel's transformation, we obtain the following boundary conditions for $z = z_0$:

$$
\begin{aligned}
\hat{e} - 2kGq &= b \\
\hat{\chi} - 2kGw &= 0
\end{aligned}
\tag{13}
$$

where

$$
b = k\int_0^\infty r\sigma_{zz}(r)J_0(kr)\,dr \tag{14}
$$

Consider the action of a vertical force with the amplitude P_0 uniformly distributed over a circular area of radius R on the surface of a half-space ($z = z_0$). The right side, b, of the first equation (13) will be as follows:

$$
b = -\frac{P_0}{\pi R}J_1(kR) \tag{15}
$$

The condition of absence of sources at infinity ($z \to \infty$) must be added to relationships (13). Let $\hat{\chi}_j$, $\hat{e}_j$, w_j, q_j ($j = 1, 2$) be two linearly independent particular solutions of system (12) that satisfy conditions at infinity. Introducing two arbitrary coefficients $A_1(k)$ and $A_2(k)$ we obtain according to equation (13) the following equations for determination of these coefficients:

$$
\begin{aligned}
&c_{11}A_1 + c_{12}A_2 = b, \qquad c_{21}A_1 + c_{22}A_2 = 0 \\
&c_{1j} = \hat{e}_j(z_0) - 2kG(z_0)q_j(z_0), \qquad c_{2j} = \hat{\chi}_j(z_0) - 2kG(z_0)w_j(z_0)
\end{aligned}
\tag{16}
$$

After obtaining the values of $A_1(k)$ and $A_2(k)$, the amplitudes of displacements can be expressed in terms of the integrals over the parameter k (see equation (5)):

$$
\begin{aligned}
u_r &= \int_0^\infty [A_1(k)q_1(z,k) + A_2(k)q_2(z,k)]J_1(kr)\,dk \\
&= -\frac{P_0}{\pi R}\int_0^\infty J_1(kR)J_1(kr)\frac{c_{22}q_1(z,k) - c_{21}q_2(z,k)}{D}\,dk \\
u_z &= \int_0^\infty [A_1(k)w_1(z,k) + A_2(k)w_2(z,k)]J_0(kr)\,dk \\
&= -\frac{P_0}{\pi R}\int_0^\infty J_1(kR)J_0(kr)\frac{c_{22}w_1(z,k) - c_{21}w_2(z,k)}{D}\,dk
\end{aligned}
\tag{17}
$$

where

$$D = c_{11}c_{22} - c_{12}c_{21}$$

We now consider system (12). Let density, ρ, be constant. We differentiate the first equation with respect to z, and add the second equation multiplied by k to obtain the following result:

$$\frac{\mathrm{d}^2\hat{\chi}}{\mathrm{d}z^2} + \left(\frac{\rho\omega^2}{G} - k^2\right)\hat{\chi} - 2k\frac{\mathrm{d}G}{\mathrm{d}z}\frac{\tau^2\hat{e}}{G} - 2k\frac{\mathrm{d}^2G}{\mathrm{d}z^2}w = 0 \tag{18}$$

This equation takes an especially simple form for the incompressible material, whose shear modulus varies linearly with depth.

INCOMPRESSIBLE HALF-SPACE WITH LINEARLY VARYING SHEAR MODULUS

Consider a half-space with the shear modulus that varies linearly according to the law

$$G(z) = mz \quad (z_0 \leqslant z < \infty) \tag{19}$$

where m is a positive constant of dimension of the force divided by the length cubed; the origin of co-ordinates is above the surface of the half-space and z-axis is directed toward the half-space. The constant m can be written in the form $m = G(z_0)/z_0$, where z_0 corresponds to z at the surface. It is appropriate to introduce into the solution dissipative properties of the material. For the harmonic motion one can consider the shear modulus as a complex quantity. Following the widely used approach, we adopt

$$G(z_0) = G_0(1 + \mathrm{i}\varepsilon), \qquad m = m_0(1 + \mathrm{i}\varepsilon), \quad m_0 = G_0/z_0 \tag{20}$$

where ε is a small positive constant and G_0 is the shear modulus at the surface for the non-dissipative case. Poisson's ratio is assumed to be real.

For the considered half-space, equation (18) can be written as follows:

$$\frac{\mathrm{d}^2\hat{\chi}}{\mathrm{d}\zeta^2} - \left(\frac{1}{4} - \frac{\gamma}{\zeta}\right)\hat{\chi} = 0 \tag{21}$$

where

$$\zeta = 2kz, \quad \gamma = \frac{\beta^2\theta^2}{2\tilde{k}}, \quad \beta = (1 + \mathrm{i}\varepsilon)^{-1/2}, \quad \theta = \omega z_0(\rho/G_0)^{1/2}, \quad \tilde{k} = kz_0$$

System (12) takes the form

$$\begin{aligned}
\frac{\mathrm{d}\hat{\chi}}{\mathrm{d}\zeta} &= \frac{\hat{e}}{2} + m(w - \gamma q)\\
\frac{\mathrm{d}\hat{e}}{\mathrm{d}\zeta} &= \frac{\hat{\chi}}{2} + m(q - \gamma w)\\
\frac{\mathrm{d}q}{\mathrm{d}\zeta} &= \frac{\hat{\chi}}{m\zeta} - \frac{w}{2}\\
\frac{\mathrm{d}w}{\mathrm{d}\zeta} &= -\frac{q}{2}
\end{aligned} \tag{22}$$

The two last equations result in

$$\frac{\mathrm{d}^2w}{\mathrm{d}\zeta^2} - \frac{w}{4} = -\frac{\hat{\chi}}{2m\zeta} \tag{23}$$

The one of two above-mentioned solutions (see equations (17)) is

$$\hat{\chi}_1 = 0,\ w_1 = q_1 = \exp(-\zeta/2),\ \hat{e}_1 = 2m(\gamma - 1)\exp(-\zeta/2) \tag{24}$$

where the expression for $\hat{e}_1$ is obtained from the first equation (22).

To construct the second solution, we use equation (21) which is a particular case of Whittaker's differential equation.[17] To fulfil the condition that the solution decreases at infinity, we adopt

$$\hat{\chi}_2 = mW_{\gamma,1/2}(\zeta) = m\zeta\exp(-\zeta/2)U(1-\gamma, 2, \zeta) \tag{25}$$

where $W_{\gamma,1/2}$ is Whittaker function, and U is the confluent hypergeometric function.[17] After substituting this result in equation (23) the latter equation has the following particular solution:

$$w = \frac{1}{2\gamma} W_{\gamma,1/2}(\zeta) \tag{26}$$

In order to simplify the study the range of low frequencies, it is appropriate to add to expression (26) a term proportional to $\exp(-\zeta/2)$, which is a solution of the homogeneous equation corresponding to equation (23); note that in the solution given by Awojobi[5,6] components become infinite when the frequency tends to zero. Here we use the following expression for the function w_2:

$$w_2 = \frac{1}{2\gamma}[W_{\gamma,1/2}(\zeta) - \exp(-\zeta/2)] = \frac{\exp(-\zeta/2)}{2\gamma}[\zeta U(1-\gamma, 2, \zeta) - 1] \tag{27}$$

Note, that according to Reference 17, $U(1-\gamma, 2, \zeta) \to 1/\zeta$ when $\gamma \to 0$. For constructing the corresponding static solution, we rewrite expression (27) in the form[17]

$$w_2 = \frac{\exp(-\zeta/2)}{2}\left[U(1-\gamma, 1, \zeta) + \frac{U(-\gamma, 1, \zeta) - 1}{\gamma}\right] \tag{28}$$

Using the series representation[17] for the function $U(-\gamma, 1, \zeta)$ it can be shown that the limit of the second term in square brackets is $\ln(\zeta)$ when $\gamma \to 0$. Thus, for the static case we obtain

$$w_2^{st} = \frac{\exp(-\zeta/2)}{2}[U(1, 1, \zeta) + \ln(\zeta)] \tag{29}$$

The expression for q_2 can be obtained in accordance with the last equation (22) using relationships for Whittaker functions and confluent hypergeometric functions:[17]

$$q_2 = w_2 - \exp(-\zeta/2)U(1-\gamma, 1, \zeta) \tag{30}$$

The corresponding result for the static case is

$$q_2^{st} = 0{\cdot}5\exp(-\zeta/2)[\ln(\zeta) - U(1, 1, \zeta)] \tag{31}$$

The expression for $\hat{e}$ is defined from the first equation (22). After transformation one can obtain

$$\hat{e}_2 = -m\exp(-\zeta/2) - 2mw_2 \tag{32}$$

with the following static result:

$$\hat{e}_2^{st} = -m\exp(-\zeta/2)[1 + U(1, 1, \zeta) + \ln(\zeta)] \tag{33}$$

The second static solution for $\hat{\chi}$ follows from equation (25):

$$\hat{\chi}_2^{st} = m\exp(-\zeta/2) \tag{34}$$

while according to solution (24)

$$\hat{\chi}_1^{\mathrm{st}} = 0, \qquad w_1^{\mathrm{st}} = q_1^{\mathrm{st}} = \exp(-\zeta/2), \qquad \hat{e}_1^{\mathrm{st}} = 2m\exp(-\zeta/2)$$

Inserting the above solutions and using relationships from Reference 17 for confluent hypergeometric functions, expressions for displacements (17) can be represented in the form

$$\begin{aligned} u_r &= \frac{P_0\beta^2}{2\pi R G_0}\int_0^\infty \mathrm{e}^{-\tilde{k}(\bar{z}-1)} J_1(\tilde{k}\bar{R}) J_1(\tilde{k}\bar{r}) \frac{F_r}{\tilde{D}}\,\mathrm{d}\tilde{k} \\ u_z &= \frac{P_0\beta^2}{2\pi R G_0}\int_0^\infty \mathrm{e}^{-\tilde{k}(\bar{z}-1)} J_1(\tilde{k}\bar{R}) J_0(\tilde{k}\bar{r}) \frac{F_z}{\tilde{D}}\,\mathrm{d}\tilde{k} \end{aligned} \tag{35}$$

where

$$\begin{aligned} &\bar{r} = r/z_0, \qquad \bar{R} = R/z_0, \qquad \bar{z} = z/z_0, \\ &\tilde{D} = [\gamma(2\tilde{k} + 1 - \gamma) - 2\tilde{k}^2]U(1-\gamma, 1, 2\tilde{k}) + (2\tilde{k} + 1 - \gamma)U(-\gamma, 1, 2\tilde{k}) \\ &F_r = (\gamma - \tilde{k})U(1-\gamma, 1, 2\tilde{k}) + U(-\gamma, 1, 2\tilde{k}) - \tilde{k}U(1-\gamma, 1, 2\tilde{k}\bar{z}) - \tilde{k}[\Phi(2\tilde{k}) - \Phi(2\tilde{k}\bar{z})] \\ &F_z = (\gamma - \tilde{k})U(1-\gamma, 1, 2\tilde{k}) + U(-\gamma, 1, 2\tilde{k}) + \tilde{k}U(1-\gamma, 1, 2\tilde{k}\bar{z}) - \tilde{k}[\Phi(2\tilde{k}) - \Phi(2\tilde{k}\bar{z})] \\ &\Phi(\eta) = \frac{U(-\gamma, 1, \eta) - 1}{\gamma} \end{aligned} \tag{36}$$

For the static case

$$\begin{aligned} \tilde{D}^{\mathrm{st}} &= 2\tilde{k} + 1 - 2\tilde{k}^2 U(1, 1, 2\tilde{k}) \\ F_r^{\mathrm{st}} &= 1 - \tilde{k}U(1, 1, 2\tilde{k}) - \tilde{k}U(1, 1, 2\tilde{k}\bar{z}) + \tilde{k}\ln(\bar{z}) \\ F_z^{\mathrm{st}} &= 1 - \tilde{k}U(1, 1, 2\tilde{k}) + \tilde{k}U(1, 1, 2\tilde{k}\bar{z}) + \tilde{k}\ln(\bar{z}) \end{aligned} \tag{37}$$

The result obtained for u_z^{st} is in accordance with the corresponding result of Gibson.[1] Note that function $U(1, 1, \eta)$ can be represented by the exponential integral function used in Reference 1.

Consider the case of zero shear modulus on the surface of the half-space. Taking limits in equations (35) when $z_0 \to 0$, $G_0 \to 0$ ($m_0 \neq 0$), we can write

$$\begin{aligned} \tilde{D} &\approx (1-\gamma)[\gamma U(1-\gamma, 1, 2kz_0) + U(-\gamma, 1, 2kz_0)] \\ F_r &\approx F_z \approx \gamma U(1-\gamma, 1, 2kz_0) + U(-\gamma, 1, 2kz_0) \end{aligned} \tag{38}$$

Thus, the solution for the considered case will be

$$\begin{aligned} u_r &= \frac{P_0\beta^2}{2\pi R m_0}\int_0^\infty \mathrm{e}^{-kz}\frac{J_1(kR)J_1(kr)}{1-\gamma}\,\mathrm{d}k \\ u_z &= \frac{P_0\beta^2}{2\pi R m_0}\int_0^\infty \mathrm{e}^{-kz}\frac{J_1(kR)J_0(kr)}{1-\gamma}\,\mathrm{d}k \end{aligned} \tag{39}$$

For $\gamma = 0$ these expressions represent the static solution for the case of zero shear modulus at the surface; the result for u_z is in agreement with the corresponding Gibson's[1] result. The consideration of the expression for u_r shows that displacements at the surface tend to infinity when $r \to R$. In fact, for $r = R$ and for large values of k

$$J_1(kR)J_1(kr) \approx \frac{1 - \sin(2kR)}{\pi kR} \tag{40}$$

and convergence of the integral disappears if $z = 0$. This result restricts the application of the considered model (with zero surface modulus) for practical purposes.

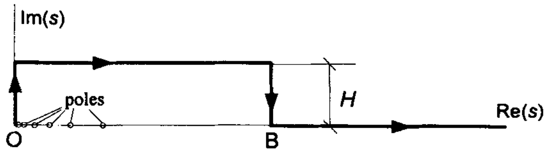

Figure 1. Contour of integration

Further, the case $z_0 > 0$ will be studied. Consider displacements at the surface of the half-space. Due to recurrence relations[17] for functions U, equations (36) simplify to

$$\begin{aligned} F_r &= 2\tilde{k}U(1-\gamma, 2, 2\tilde{k}) - 2\tilde{k}U(1-\gamma, 1, 2\tilde{k}) \\ F_z &= 2\tilde{k}U(1-\gamma, 2, 2\tilde{k}) \end{aligned} \tag{41}$$

The relations $F_r/\tilde{D}$ and $F_z/\tilde{D}$ can be rewritten as follows:

$$\frac{F_r}{\tilde{D}} = \frac{1-\Psi(2\tilde{k})}{2\tilde{k}+1-\gamma-\tilde{k}\Psi(2\tilde{k})}, \qquad \frac{F_z}{\tilde{D}} = \frac{1}{2\tilde{k}+1-\gamma-\tilde{k}\Psi(2\tilde{k})} \tag{42}$$

where

$$\Psi(\eta) = \frac{U(1-\gamma, 1, \eta)}{U(1-\gamma, 2, \eta)} \tag{43}$$

Using asymptotic expansions for confluent hypergeometric functions,[17] one can obtain the following representations for large values of $\tilde{k}$:

$$\frac{F_r}{\tilde{D}} \approx \frac{1}{2\tilde{k}^2}, \qquad \frac{F_z}{\tilde{D}} \approx \frac{1}{\tilde{k}} \tag{44}$$

If the integration parameter $\tilde{k}$ tends to zero, the parameter γ increases without limit (for the time-harmonic case) which results in oscillations of integrands in equations (35) and, as the calculations show, the poles of integrands appear in great numbers on the real axis of the complex plane for the non-dissipative half-space. Number of poles tends to be infinite as the zero point of $\tilde{k}$ is approached. We introduce the damping parameter ε (see equation (20)) to shift the poles down. Therefore, it is convenient to use the contour of integration shown in Figure 1, where H is a small quantity, and the point B lies to the right of all the singularities and its abscissa is large enough for application of asymptotic representations of Bessel functions in equations (35). In Figure 2, the variation of the value of $\bar{w} = \tilde{k}F_z/\tilde{D}$ is presented on a line, which is parallel to the real axis of the complex plane, for the value of the parameter $\theta = 10$ ($\varepsilon = 0$). The variable $s = \tilde{k}/\theta$ is used instead of $\tilde{k}$; $s = \mathrm{Re}(s) + \mathrm{i}H_s$ where the value H_s denotes the shifting of the contour for the variable s. When $\theta \neq 0$, the substitution $s = \tilde{k}/\theta$ is appropriate for integrating equations (35). This leads to locating the area with poles on the interval $0 < \mathrm{Re}(s) < 1{\cdot}2$ (for θ till 20). In the static case, the former variable $\tilde{k}$ is used.

The numerical results correspond to the case of the point force ($R \to 0$); in this case the value of $J_1(\tilde{k}\bar{R})/R$ in the integrals is replaced with $0{\cdot}5\tilde{k}/z_0$, and the expressions for the displacements at the surface can be rewritten as follows:

$$\begin{aligned} u_r &= \frac{P_0}{4G_0\pi r} S_{vh}, \qquad u_z = \frac{P_0}{4G_0\pi r} S_{vv} \\ S_{vh} &= \beta^2 \bar{r} \int_0^\infty \frac{\tilde{k}[1-\Psi(2\tilde{k})]}{2\tilde{k}+1-\gamma-\tilde{k}\Psi(2\tilde{k})} J_1(\tilde{k}\bar{r})\,\mathrm{d}\tilde{k} \\ S_{vv} &= \beta^2 \bar{r} \int_0^\infty \frac{\tilde{k}}{2\tilde{k}+1-\gamma-\tilde{k}\Psi(2\tilde{k})} J_0(\tilde{k}\bar{r})\,\mathrm{d}\tilde{k} \end{aligned} \tag{45}$$

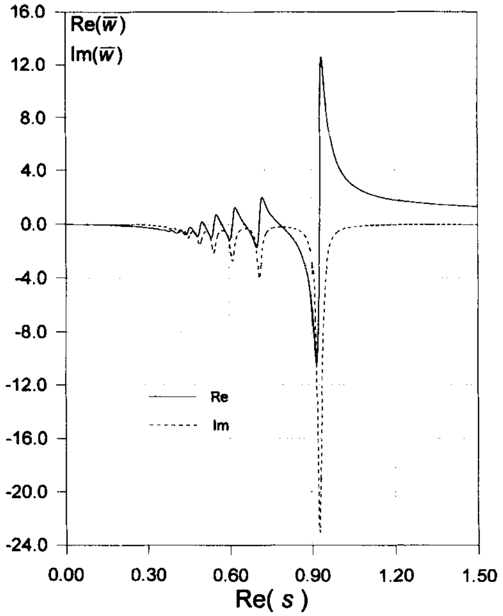

Figure 2. The value $\bar{w}(s) = \tilde{k}F_z/\tilde{D}$ versus Re(s) for $\theta = 10$ and for the contour shifting $H_s = 0{\cdot}01$.

In the expressions for u_r and u_z, the values of S_{vh} and S_{vv} are multiplied by the coefficient that corresponds to vertical static displacements for the homogeneous incompressible half-space (the horizontal displacements for such a half-space are equal to zero). The parts of the integrals corresponding to the interval $B < \tilde{k} < \infty$ are evaluated by means of the integration by parts after using the asymptotic representation for Bessel functions

$$J_n(\tilde{k}\bar{r}) \approx [2/(\pi\tilde{k}\bar{r})]^{1/2} \cos(\tilde{k}\bar{r} - n\pi/2 - \pi/4) \tag{46}$$

In order to improve the convergence of integrals, it is appropriate to use the results given in equations (44). The corresponding limit values of the multipliers before Bessel functions in integrands in equations (45) will be $1/(2\tilde{k})$ and 1 for u_r and u_z, respectively. Subtracting and adding these values, we can use the known integrals

$$\int_0^\infty \frac{J_1(x)}{x}\,\mathrm{d}x = 1, \quad \int_0^\infty J_0(x)\,\mathrm{d}x = 1 \tag{47}$$

for evaluating the amplitudes of vibrations in equations (45).

First consider the static case. Using equation (45) we set

$$\gamma = 0, \quad \beta = 1, \quad \Psi(2\tilde{k}) = 2\tilde{k}U(1, 1, 2\tilde{k}) \tag{48}$$

Results of calculations are shown in Figure 3. The normalized values S^{st}_{vh} and S^{st}_{vv} are presented as functions of the ratio $\bar{r} = r/z_0$ which shows how significantly the non-homogeneity influences the displacements. As to the horizontal displacements, they are equal to zero for the incompressible homogeneous half-space (at the surface), whereas for the non-homogeneous half-space the horizontal displacements can surpass considerably the vertical displacements at large distances from the force.

In the dynamic case, the frequency parameter $a = \omega r(\rho/G_0)^{1/2}$ is used instead of $\bar{r}$. Figures 4 and 5 show the behavior of the real and imaginary parts of amplitudes of vibration for $\varepsilon = 0$ in equation (20). As seen, with the increase of the parameter θ, the solutions approach the homogeneous solution. Vertical displacements for $\varepsilon = 0{\cdot}05$ are represented in Figure 6, which shows that relationships between results for the

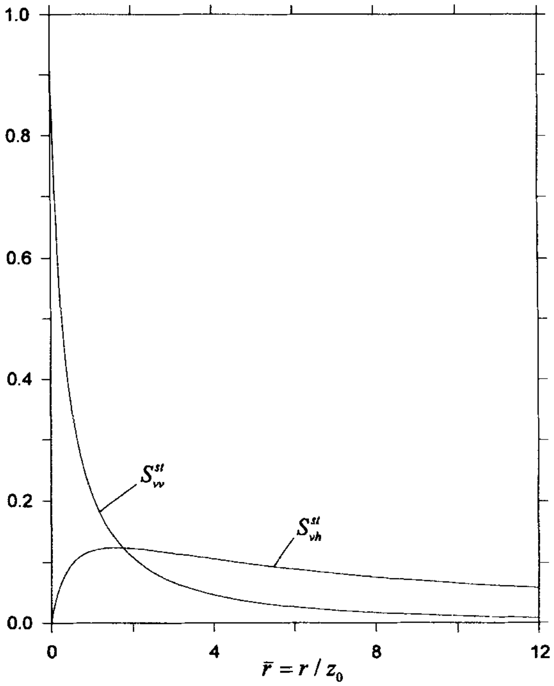

Figure 3. Normalized static vertical and horizontal surface displacements of the non-homogeneous half-space due to a vertical surface point force

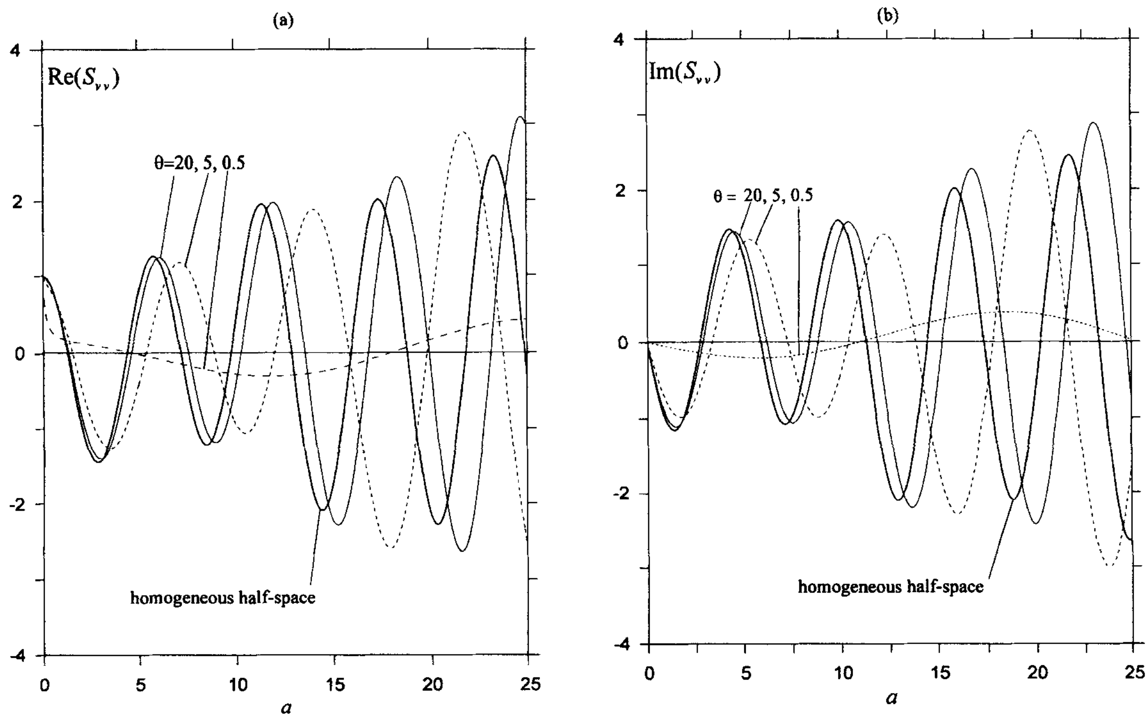

Figure 4. Real part (a) and imaginary part (b) of normalized vertical surface displacements, caused by a vertical surface point force versus frequency parameter a for $\varepsilon = 0$ and for some values of the parameter θ reflecting degree of non-homogeneity

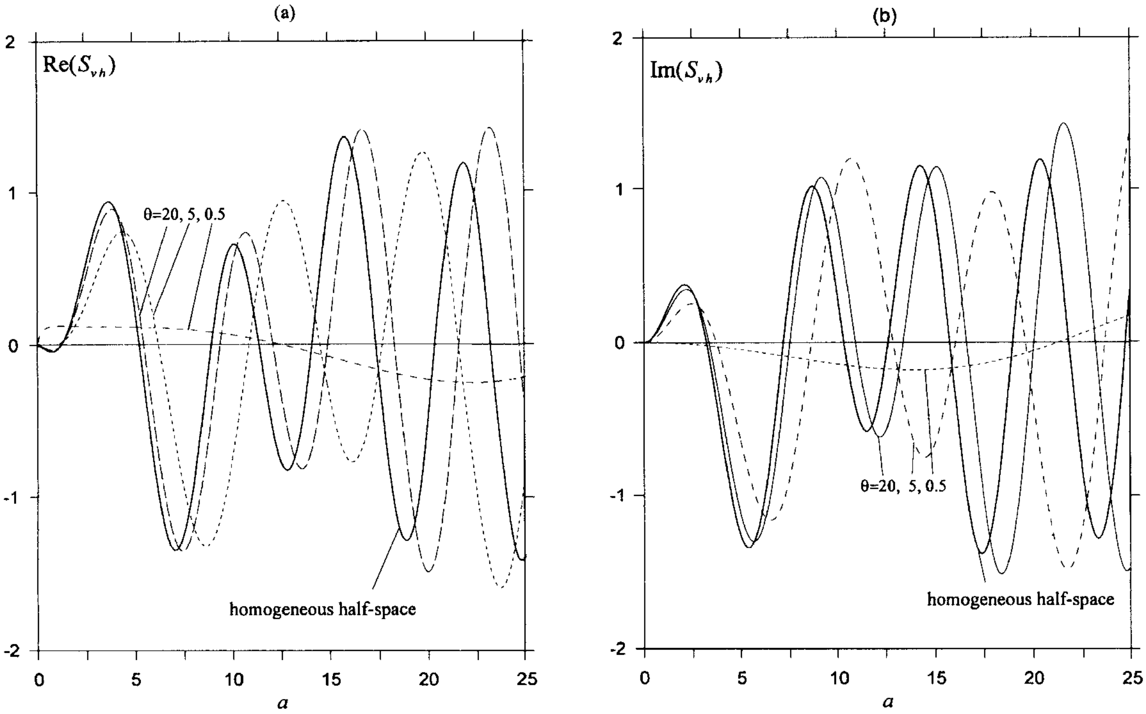

Figure 5. Real part (a) and imaginary part (b) of normalized horizontal surface displacements, caused by a vertical surface point force versus frequency parameter a for $\varepsilon = 0$ and for some values of the parameter θ

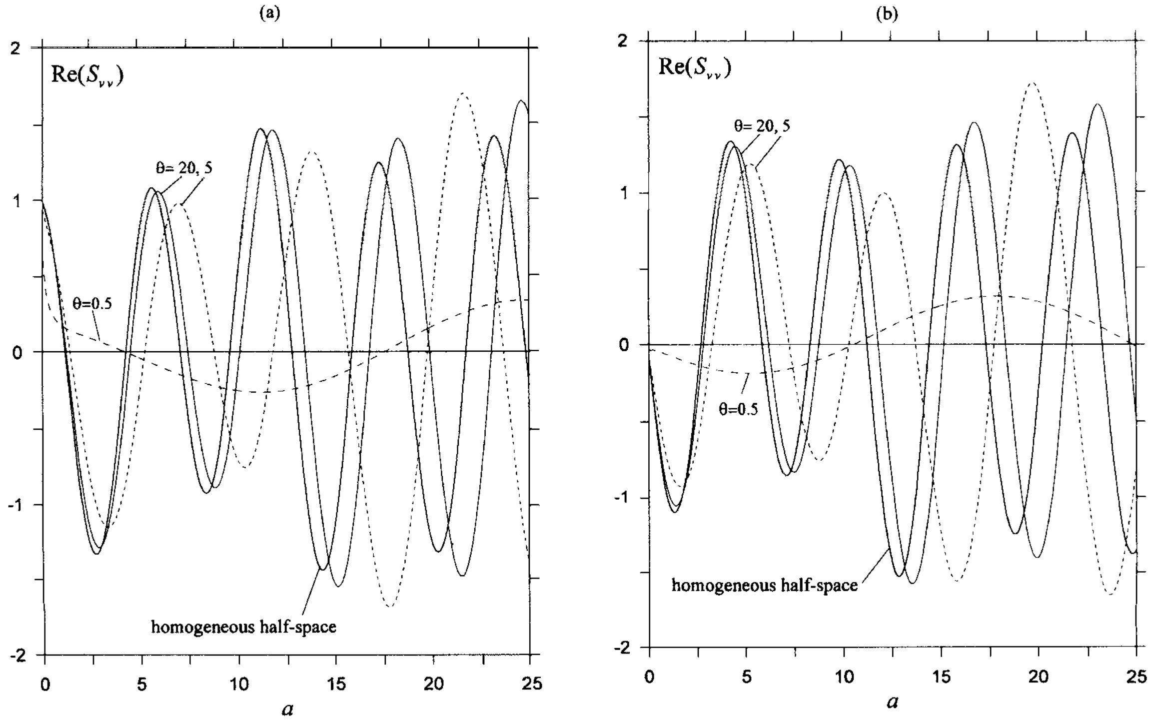

Figure 6. Real part (a) and imaginary part (b) of normalized vertical surface displacements, caused by a vertical surface point force versus frequency parameter a for $\varepsilon = 0{\cdot}05$ and for some values of the parameter θ

homogeneous and for the non-homogeneous cases are similar to those for the non-dissipative material. The results show that for large distances from the acting force the amplitudes at the surface of the non-homogeneous half-space can noticeably exceed the corresponding amplitudes for the homogeneous half-space.

One of the important problems in foundation dynamics is the evaluation of the stiffness of the loaded area. Having the solution corresponding to a vertical point force applied to the surface of the half-space one can study vertical vibrations of a rigid body lying on the half-space. In the axisymmetric case of a circular disk, assuming smooth contact, the desired solution can be obtained by dividing the contact area into a number of annular subrings and introducing unknown pressures, assumed to be constant on each element. As the contact pressure tends to infinity in the vicinity of the edge of the contact area, the increase of the widths of elements is used in the direction from the boundary to the centre of the disk. For the number of elements $n = 20$, the increase according to the geometrical progression with the common ratio $q = 1{\cdot}1$ is used. The precision was checked by means of the known solution for the static problem for the homogeneous half-space and solutions corresponding to the value $n = 40$. The result for the uniform load applied to an annular ring is obtained immediately when the corresponding result for the circular area is known. Although the expression corresponding to a circular area is available (see equations (35)), it seems more appropriate to apply the superposition principle using the solution for the point force, analysed numerically in the foregoing. The following expression is used for calculating the vertical amplitudes, $w(r)$, corresponding to vertical time-harmonic load P_0, uniformly distributed over a circular area of radius R on the surface of the half-space[18]

$$w(r) = \frac{2}{\pi}\int_{|\eta-1|}^{\eta+1} xu_z(xR)\arccos\frac{x^2+\eta^2-1}{2x\eta}\,\mathrm{d}x \quad \left(\eta = \frac{r}{R} \geqslant 1\right) \tag{49}$$

where r is the distance of the considered point from the centre of the loaded area, u_z is given by equation (45). The value xR in equation (49) is substituted for argument r in the expression for u_z. If $\eta < 1$ then the following value

$$2\int_0^{1-\eta} xu_z(xR)\,\mathrm{d}x \tag{50}$$

should be added to expression (49).

The pressures on the elements are calculated on the basis of the requirement that the vertical amplitudes in middle points of the elements be equal to the amplitude of disk vibration. The total load found through calculated pressures corresponding to the unit disk amplitude gives the value of dynamic stiffness of the massless disk foundation with smooth footing.

First consider the static stiffness. Let R denote the radius of the disk and $\bar{R} = R/z_0$, as above. It is appropriate to use the value $\lambda = (1+\bar{R})^{-1}$ as an independent variable for graphical presentation of the results. The variable λ is equal to the ratio of the shear modulus at the surface of the half-space to the shear modulus at the depth R (see Reference 3). The value $\lambda = 0$ ($z_0 \to 0$, $\bar{R} \to \infty$) corresponds to zero shear modulus at the surface of the half-space when the surface behaves as Winkler's base[1] with the coefficient of subgrade reaction $k_s = 2m_0$. In this case the static stiffness is equal to $2m_0\pi R^2$. In Figure 7 the normalized static stiffness $\tilde{K}^{st}$ is presented which is defined as

$$\tilde{K}^{st} = \frac{k^{st}}{k^{st}_{hm}}, \quad k^{st}_{hm} = \frac{4\tilde{G}R}{1-\nu} = 8\tilde{G}R, \; \tilde{G} = G_0(1+\bar{R}) \tag{51}$$

where k^{st} is the calculated static stiffness, k^{st}_{hm} is the static stiffness of the rigid disk on the incompressible homogeneous half-space with the shear modulus $\tilde{G}$, which is equal to the shear modulus of the non-homogeneous half-space at the depth of R. The value k^{st}_{hm} can be found in Reference 15. Note that for the case $\lambda = 0$ we have $\tilde{G} = m_0R$, $\tilde{K}^{st} = \pi/4$. The results presented in Figure 7 are in agreement with those of Brown.[3] Note that in Figure 7, the calculated quantity corresponding to the value of $\lambda = 1$ (homogeneous half-space)

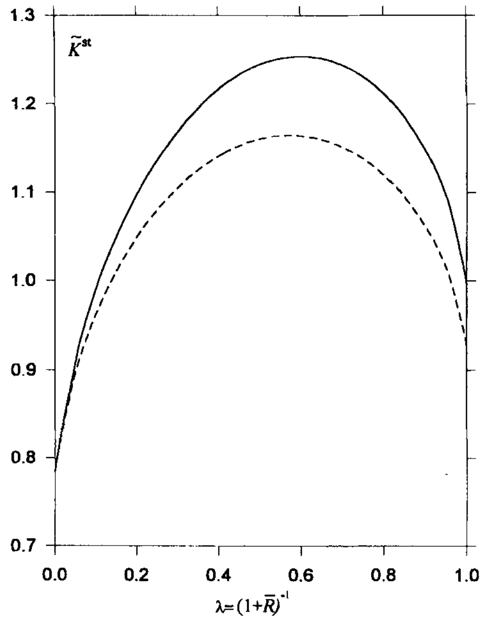

Figure 7. Normalized vertical static stiffness of the disk foundation: the solid line is for the rigid disk condition; the dashed line corresponds to averaging of the displacements caused by a uniform load

is equal to 0·996 instead of $1(n = 20,\ q = 1{\cdot}1)$; for $n = 40$, $q = 1{\cdot}05$, the corresponding value is 0·998. In addition, the solution, which corresponds to averaging vertical displacements of points in the circular area subjected to a uniform distributed pressure, is presented by a dashed line. According to Reference 18, the mean value Δ_z, defined as the integral of displacements over the loaded region divided by the area of the region, can be expressed in the form

$$\Delta_z = \frac{2}{\pi R^2}\int_0^2 W(xR)(4-x^2)^{1/2}\,\mathrm{d}x = \frac{2}{\pi}\int_0^2 xu_z(xR)[\pi - 0{\cdot}5x(4-x^2)^{1/2} - 2\arcsin(x/2)]\,\mathrm{d}x \tag{52}$$

where

$$W(h) = \int_0^h u_z(r)r\,\mathrm{d}r \tag{53}$$

As seen from Figure 7, the averaging gives results that are acceptable for engineering practice (an error in the stiffness does not exceed 8·5 per cent) and has the advantage of simplicity in comparison to the solution satisfying rigid disk conditions. Apparently, this treatment should be relevant also for time-harmonic problems at low frequencies.

The results concerning the dynamic stiffness are presented in Figure 8. The value $\tilde{a}_0 = \omega R(\rho/\tilde{G})^{1/2}$ is used as the frequency parameter. The normalized stiffness K is defined as the dynamic stiffness divided by the corresponding static stiffness presented in Figure 7. The results that correspond to solution (39) (i.e. the case of zero shear modulus as the surface of the half-space ($\bar{R} \to \infty$)) are shown in Figure 8 as well. This case and the case of the homogeneous half-space present two extreme degrees of the considered type of non-homogeneity. In Figure 8 also the solution of Awojobi[5] is shown that was found for the low-frequency domain. As seen, this solution is acceptable for values of parameter $\tilde{a}_0$ less than 0·5. The graphs in Figure 8 for the real parts of the normalized dynamic stiffness corresponding to different degree of non-homogeneity are closely allied, whereas the imaginary parts are strongly influenced by non-homogeneity parameter $\bar{R}$. The main consequence of the presented results is a considerable decrease of damping.

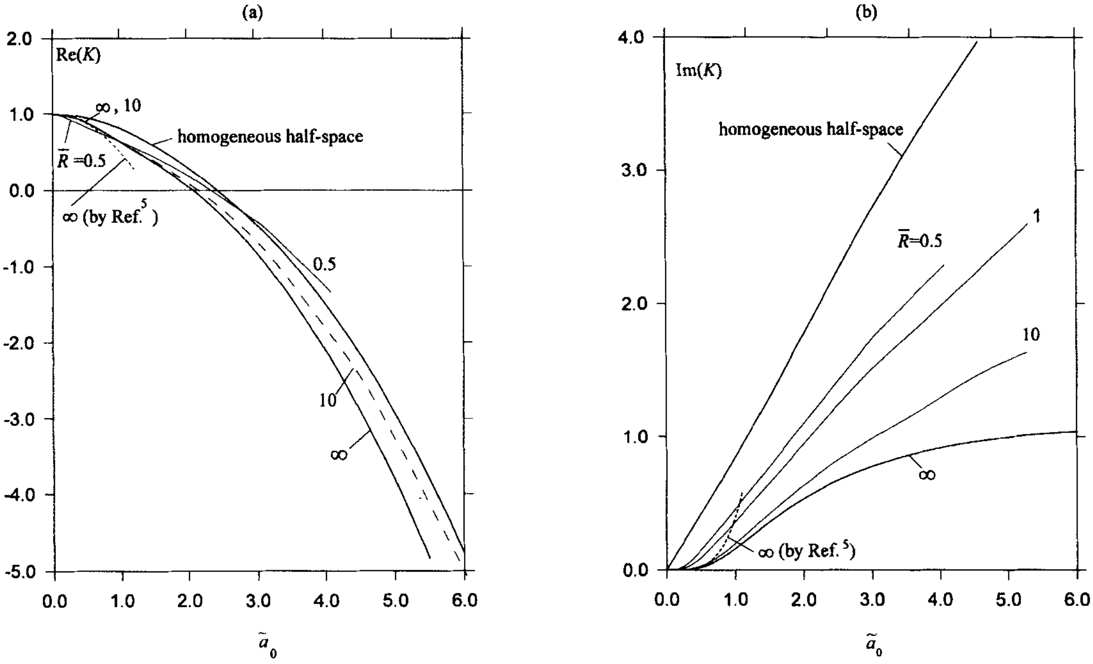

Figure 8. Real part (a) and imaginary part (b) of the normalized vertical dynamic stiffness of the rigid disk foundation versus frequency parameter $\tilde{a}_0$ for $\varepsilon = 0$ and for some values of the parameter $\bar{R}$

CONCLUSIONS

This paper presents the solution of the time-harmonic axisymmetric problem for the incompressible viscoelastic linearly non-homogeneous half-space subjected to vertical surface forces. It is shown how difficulties, associated with the infinite number of poles of Hankel's transforms of the solution, can be avoided by the proper shifting of the path of integration. The numerical results relating to surface displacements cuased by a point force are presented for a wide range of variation of frequency and degree of non-homogeneity. The non-homogeneity reduces the radiation of energy into the half-space compared to the homogeneous case. Thus, amplitudes of vertical vibration of points at the surface of the non-homogeneous half-space at large distances from the acting point force exceed noticeably (for some values of the parameter of non-homogeneity θ) the amplitudes for the homogeneous half-space with the same shear modulus at the surface, despite the fact that in this comparison the non-homogeneous half-space is stiffer. The decrease of damping is exhibited also in the results corresponding to vertical vibrations of a rigid circular disk. For representation of numerical results, we consider half-spaces with the same shear modulus at depth of the disk radius. For these half-spaces, values of the static stiffness are relatively close together (Figure 7) as well as the real parts of the dynamic stiffness (Figure 8). However, the imaginary parts of the dynamic stiffness, having the direct effect on the damping of foundation vibrations, remain strongly influenced by the parameter of non-homogeneity. Presented results help to evaluate damping parameters in the foundation vibrations.

REFERENCES

1. R. E. Gibson, 'Some results concerning displacements and stresses in a non-homogeneous elastic half-space', *Geotechnique* **17**, 58–67 (1967).
2. A. O. Awojobi and R. E. Gibson, 'Plane strain and axially symmetric problems of a linearly nonhomogeneous elastic half-space', *Q. j. mech. appl. math.* **26**, 285–302 (1973).
3. P. T. Brown, Influence of soil inhomogeneity on raft behaviour, *Soil Found.* **14**, 61–70 (1974).
4. J. P. Dempsey and H. Li, 'Rectangular footing on nonhomogeneous elastic half-space', in F. H. Kulhawy (ed.), *Foundation Engineering: Current Principles and Practices ASCE*, Vol. 2, ASCE, New York, 1989, pp 1212–1225.

5. A. O. Awojobi, 'Vertical vibration of a rigid circular foundation on Gibson soil', *Geotechnique* **22**, 333–343 (1972).
6. A. O. Awojobi, 'Vibration of rigid bodies on non-homogeneous elastic semi-infinite elastic media', *Q. j. mech. appl. math.* **26**, 483–498 (1973).
7. R. Stoneley, 'The transmission of Rayleigh waves in a heterogeneous medium', *Geophysical suppl. to the monthly notices of the Roy. astron. soc.*, London **3**, 222–232 (1934).
8. I. Vardoulakis, 'Surface waves in a half-space of submerged sand', *Earthquake eng. struct. dyn.* **9**, 329–342 (1981).
9. I. Vardoulakis and C. Vrettos, 'Dispersion-law of Rayleigh-type waves in a compressible Gibson half-space', *Int. j. numer. anal. methods geomech.* **12**, 639–655 (1988).
10. G. Waas, H. R. Riggs and H. Werkle, 'Displacements solutions for dynamic loads in transversely-isotropic stratified media', *Earthquake eng. struct. dyn.* **13**, 329–342 (1985).
11. E. Kausel and R. Peek, 'Dynamic loads in the interior of a layered stratum: an explicit solution', *Bull. seism. soc. Am.* **72**, 1459–1481 (1982). Also Errata, ibid. **74**, 1508 (1984).
12. J. E. Luco and R. J. Apsel, 'On the Green's functions for a layered half-space. Part I', *Bull. seism. soc. Am.* **73**, 909–929 (1983).
13. R. J. Apsel and J. E. Luco, 'On the Green's functions for a layered half-space. Part II', *Bull. seism. soc. Am.* **73**, 931–951 (1983).
14. F. Chapel, 'Boundary element method applied to linear soil–structure interaction on a heterogeneous soil', *Earthquake eng. struct. dyn.* **15**, 815–829 (1987).
15. J. P. Wolf, *Dynamic Soil–Structure Interaction*, Prentice-Hall, Englewood Cliffs, NJ, 1985.
16. C. Vrettos, 'Time-harmonic Boussinesq problem for a continuously non-homogeneous soil', *Earthquake eng. struct. dyn.* **20**, 961–977 (1991).
17. M. Abramowitz and I. A. Stugun, *Handbook of Mathematical Functions*, Dover, New York, 1964.
18. G. B. Muravskii, 'Equations for the integral mean values of the displacements of linearly deformable foundation beds', *Soil mech. found. eng.* (translated from Russian) **8**, 14–19 (1971).